PHYSICAL REVIEW B **92**, 241118(R) (2015)

Pressure-induced quantum phase transitions in a YbB_6 single crystal

Yazhou Zhou,[1] Dae-Jeong Kim,[2] Priscila Ferrari Silveira Rosa,[2] Qi Wu,[1] Jing Guo,[1] Shan Zhang,[1] Zhe Wang,[1] Defen Kang,[1] Wei Yi,[1] Yanchun Li,[3] Xiaodong Li,[3] Jing Liu,[3] Peiquan Duan,[4] Ming Zi,[4] Xiangjun Wei,[4] Zheng Jiang,[4] Yuying Huang,[4] Yi-feng Yang,[1,5] Zachary Fisk,[2] Liling Sun,[1,5,*] and Zhongxian Zhao[1,5]

[1]*Institute of Physics, Beijing National Laboratory for Condensed Matter Physics, Chinese Academy of Sciences, Beijing 100190, China*

[2]*Department of Physics and Astronomy, University of California, Irvine, California 92697, USA*

[3]*Institute of High Energy Physics, Chinese Academy of Sciences, Beijing 100049, China*

[4]*Shanghai Synchrotron Radiation Facilities, Shanghai Institute of Applied Physics, Chinese Academy of Sciences, Shanghai 201204, China*

[5]*Collaborative Innovation Center of Quantum Matter, Beijing 100190, China*

(Received 14 February 2015; revised manuscript received 27 November 2015; published 29 December 2015)

We report the observation of two pressure-induced quantum phase transitions in a YbB_6 single crystal, i.e., from a topologically trivial semiconductor to an intermediate semimetal and then from the semimetal to a possible topologically nontrivial high-pressure gapped phase through *in situ* high-pressure transport and synchrotron x-ray diffraction measurements. Our high-pressure absorption results reveal that the mixed-valence state in pressurized YbB_6 above 15 GPa plays an important role in the formation of the high-pressure state with a reopened gap. These high-pressure results may be helpful for shedding light on the intriguing relation between the topology and the 4*f* electrons in the rare-earth hexaborides.

DOI: 10.1103/PhysRevB.92.241118 PACS number(s): 71.30.+h, 71.55.Ak, 74.62.Fj

In recent years, topological insulators (TIs) attracted intensive interests due to their nontrivial properties of coexisting insulating bulk and topologically protected conducting surfaces [1–5]. Such exotic electronic states have been observed in the compounds of Bi_2Se_3, Bi_2Te_3, and HgTe [6–10]. A new advance in the field is the possible existence of such a topological state in the rare-earth hexaborides SmB_6 and YbB_6 [11–17]. Because of containing *f* electrons, these hexaborides may exhibit a variety of exotic electronic correlation effects. In particular, they may host the novel topological electronic states that are different from the usual TIs without *f* electrons [11,15,18,19]. These hexaborides are thus expected to bridge the physics between the correlated electron material and the topological insulator. As a candidate material for the new class of TIs, ambient-pressure SmB_6 undergoes a transition from a poor metal at room temperature to a Kondo insulator (KI) with residual conductance at low temperatures [14,20,21]. Theoretical calculations point out that the low-temperature residual conductance in SmB_6 is originated from the nontrivial conducting surface state due to the hybridization between *d* orbitals and *f* orbitals of Sm ions [22]. Soon after, these predictions have been identified by many experimental measurements [12,13,17,20,21,23–36]. These results support that SmB_6 is a topological KI (TKI). For YbB_6, it crystallizes in the same structure as that of SmB_6 but presents very different electronic structures due to the fact that Yb has a fully filled 4*f* shell whereas Sm has a nearly half-filled 4*f* shell. Some results from angle-resolved photoemission spectroscopy (ARPES) measurements on the ambient-pressure YbB_6 propose that it is a topological insulator [16,37,38], whereas, other ARPES measurements argue that the YbB_6 is not a TI [39,40]. To shed light on the nature of the electronic state in ambient-pressure YbB_6 and explore its potentially new quantum phenomena, we performed high-pressure resistance, Hall coefficient, x-ray diffraction (XRD), and x-ray absorption spectroscopic (XAS) measurements on this hexaboride.

High quality single crystals of YbB_6 were grown by the Al flux method as described in Ref. [21]. Pressure was generated by a diamond-anvil cell with two opposing anvils sitting on the Be-Cu supporting plates. Diamond anvils with 400- and 300-μm flats and nonmagnetic rhenium gaskets with 200- and 100-μm diameter holes, respectively, were employed for different runs of the high-pressure studies. The four-probe method was applied on the (001) facet of single-crystal YbB_6 for all high-pressure transport measurements. To keep the sample in a quasihydrostatic pressure environment, NaCl powder was employed as the pressure medium for the high-pressure resistance, magnetoresistance, and Hall effect measurements. High-pressure XRD and XAS experiments were performed at beamline 4W2 at the Beijing Synchrotron Radiation Facility and at beamline 14W1 at the Shanghai Synchrotron Radiation Facility, respectively. Diamonds with low birefringence were selected for the experiments. A monochromatic x-ray beam with a wavelength of 0.6199 Å was adopted for all XRD measurements. To maintain the sample in a hydrostatic pressure environment, silicon oil was used as the pressure medium in the high-pressure XRD and XAS measurements. Pressure was determined by the ruby fluorescence method [41].

Figure 1 shows the results of high-pressure resistance measurements for a single-crystalline sample of YbB_6. Although the sample exhibits metallic behavior in the temperature range of 50–300 K at 0.9 GPa, at lower temperatures an insulating behavior sets in as manifested by a small upturn below 50 K [Fig. 1(a)]. This upturn is observed in three independent run measurements on samples obtained from different batches, consistent with its ambient-pressure behavior (Fig. S1 of the Supplemental Material [42]). Upon increasing pressure, the upturn is suppressed dramatically [Fig. 1(a)] and eventually goes away at ~10 GPa [Fig. 1(b)]. Subsequently, metallic resistance behavior over the entire temperature range is observed in the pressure range of 10.5–14.2 GPa [Fig. 1(b)], reflecting

*Author to whom correspondence should be addressed: llsun@iphy.ac.cn

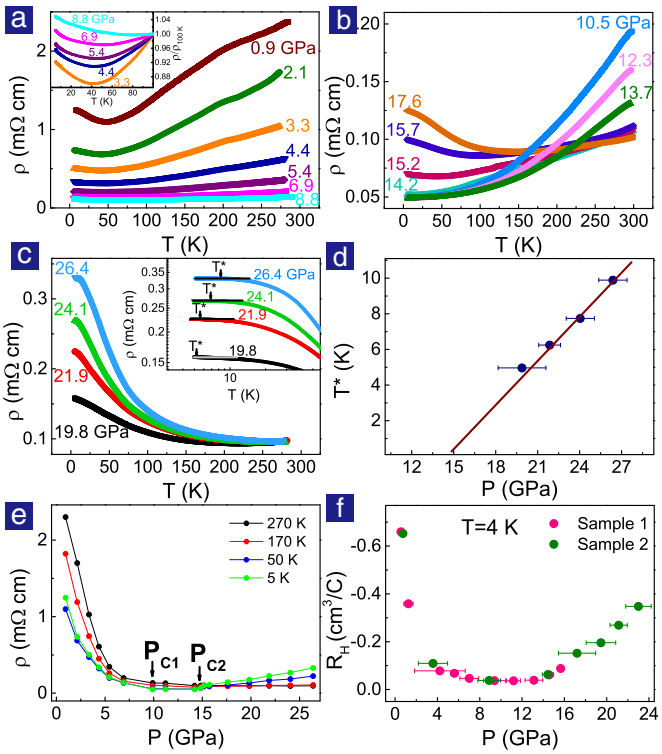

FIG. 1. (Color online) (a) Resistance-temperature (R-T) curves measured in the pressure range of 0.9–8.8 GPa, showing a remarkable pressure-induced resistance decrease over the entire temperature range. The inset displays normalized R-T curves in the low-temperature range, showing the upturns of the resistance measured at different pressures. (b) Selective R-T curves in the pressure range of 10.5–17.6 GPa, displaying a dramatic change in resistance. (c) The R-T curves measured in the pressure range of 19.8–26.4 GPa, exhibiting a significant pressure-induced enhancement of nonmetallic behavior. The inset shows the resistance plateaus (T^*) in lower temperatures at different pressures. (d) T^* as a function of pressure. (e) The pressure dependence of the resistance obtained at different fixed temperatures, illustrating two critical pressures (P_{C1} and P_{C2}). (f) Hall coefficient (R_H) as a function of pressure for single-crystal YbB_6 at 4 K.

the closure of the semiconducting gap in the bulk and the conversion from its semiconducting state into a metallic state. Upon further increasing pressure, interestingly, a resistance upturn presents at 15.2 GPa and becomes pronounced at higher pressures [Figs. 1(b) and 1(c)]. At 19.8 GPa, an apparent resistance plateau is observed at low temperatures [the inset of Fig. 1(c)], similar to what has been seen in SmB_6 [21]. The onset temperature (T^*) of the plateau shifts to higher temperatures upon increasing pressure [the insets of Figs. 1(c) and 1(d)]. Since the lowest temperature of our instrument is 4 K, we cannot detect the T^* (it should be below 4 K) for the sample subjected to pressures ranging from 15 to 19 GPa. Extrapolation of the obtained T^* down to lower pressures gives a critical pressure point at ∼15 GPa [Fig. 1(d)] where the gap is coincidently closed. To determine the critical pressures for these two phase transitions, we plot the pressure dependence of the resistance at different temperatures [Fig. 1(e)]. It is seen that the resistance at all temperatures remains nearly unchanged between 10 and 15 GPa but shows very different trends below 10 GPa and above 15 GPa, giving rise to the two critical pressures: P_{C1} (∼10 GPa), which separates the semiconducting state and the metallic state, and P_{C2} (∼15 GPa), which separates the metallic state and the high-pressure-induced state with a resistance upturn.

To further characterize these pressure-induced changes in YbB_6, we performed high-pressure Hall effect measurements. The Hall coefficient R_H measured at 4 K is plotted as a function of pressure in Fig. 1(f). The R_H displays a negative value over the entire pressure range, indicating that electron carriers are dominant in YbB_6. We find that below ∼4 GPa the absolute value of R_H decreases rapidly with increasing pressure. This remarkable decrease corresponds to the dramatic reduction in the resistance [Fig. 1(e)]. However, for pressures ranging from 10 to 15 GPa, the R_H barely changes, which may be attributed to the balance between electron and hole carrier populations, demonstrating that the intermediate phase is in a semimetallic state [43]. Significantly, an enhancing trend of R_H upon increasing pressure is observed above 15 GPa. This increase in R_H is consistent with the observed upturn behavior of the resistance [Figs. 1(b) and 1(c)].

To clarify whether the physical origin of the gap closing and reopening observed in the pressurized YbB_6 is related to a structural phase transition, we conducted high-pressure x-ray diffraction experiments for YbB_6 at beamline 4W2 at the Beijing Synchrotron Radiation Facility. We find that increasing pressure consistently pushes all Bragg peaks to a larger 2θ angle, but no new peaks appear up to 31.2 GPa [Fig. 2(a)]. The lattice parameter exhibits linear pressure dependence, and the plot of pressure-dependent volume shows no obvious discontinuity [Figs. 2(b) and 2(c)]. Earlier studies by Sidorov *et al.* [43] also found an exponential decrease in resistivity within ∼5 GPa and no structural phase transition detected by XRD measurements up to 8 GPa, in good agreement with our low-pressure results. These results rule out the possibility of a pressure-induced structural phase transition in YbB_6 and

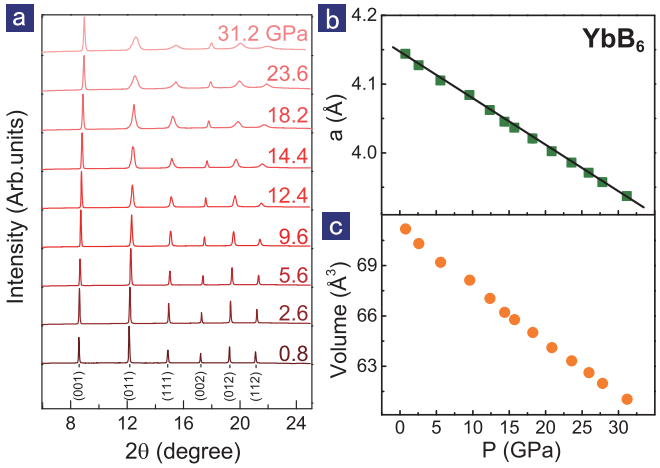

FIG. 2. (Color online) (a) X-ray diffraction patterns of YbB_6 collected at different pressures, showing that no structure phase transition occurs over the entire pressure range investigated. (b) and (c) Pressure dependences of the lattice parameter and volume of YbB_6, respectively.

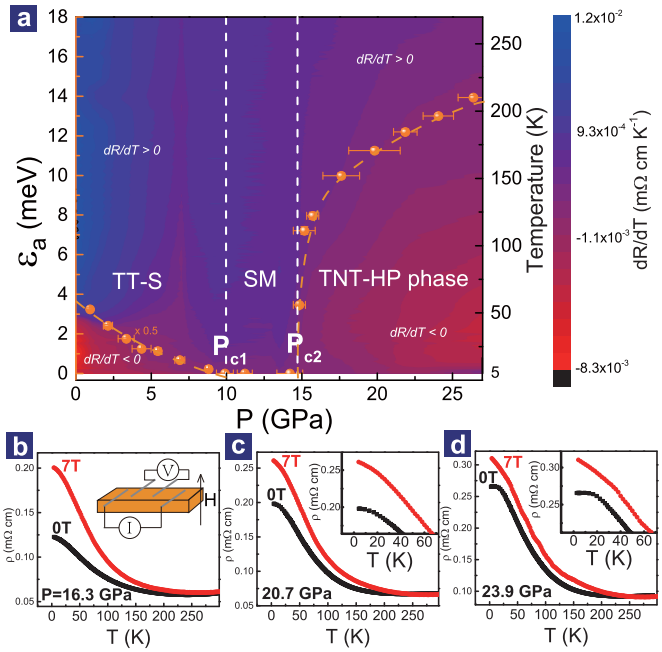

FIG. 3. (Color online) (a) Phase diagram of the pressure dependence of the activation energy gap (ε_a, left axis) and temperature (right axis) as well as the summary of dR/dT as a function of temperature and pressure. The orange solid dots represent the activation gap. The acronyms TT-S and TNT-HP phase stand for the topologically trivial semiconducting state and topologically nontrivial high-pressure gapped phase, respectively. SM represents the semimetallic state. The value of ε_a in the TT-S regime is scaled by 0.5 to fit the pressure dependence of dR/dT. (b)–(d) Temperature dependence of resistance measured at zero field and 7 T at fixed pressure. The insets illustrate the details for the measurements. The acronyms in the inset of (b), I, V, and H stand for current, voltage, and magnetic field, respectively.

indicate that the closing and reopening of the activation energy gap are of electronic origin.

The low-pressure range transport behavior of YbB_6 provides an important understanding of its ambient pressure electronic structure, a key issue for its topological nature. The combined results of the pressure-induced decline in resistivity approaching 10 GPa, the suppression of activation energy, and a constant Hall coefficient in the pressure range of 10–15 GPa provide the consistent evidence that the intermediate metallic state is a p-d overlapped semimetallic state and thus this semimetallic state should be evolved from a p-d gapped semiconducting state. This evolution has been theoretically explained, and the ambient-pressure state has been identified by ARPES measurements very recently [40].

Figure 3(a) plots dR/dT curves measured in the temperature range of 4–300 K for all pressurized samples. The activation energy (ε_a) as a function of pressure is estimated using the equation $R(T) = 1/[R_S^{-1} + R_B^{-1}\exp^{-\varepsilon_a/2k_BT}]$ where the first component is the resistance from the surface contribution and the second one is the resistance from the bulk contribution. We find a good fit to the experimental data in the two gapped regimes (Fig. S2 of the Supplemental Material). The solid dots in Fig. 3(a) are the extracted activation energy (ε_a) of the sample subjected to different pressures. It is seen that, at the base temperature, the phase diagram contains three distinct regimes. In the left regime, ε_a is reduced with increasing pressure and approaches zero at P_{C1} (~10 GPa), demonstrating that the host sample undergoes a transition from a TT-S state with a positive dR/dT in the high-temperature range and a negative dR/dT in the low-temperature range to a SM state (the middle regime). On further increasing pressure above P_{C2}, the sample moves into a novel high-pressure state with a reopened gap (the right regime).

Intriguingly, the behavior of the low-temperature resistance plateau in pressurized YbB_6 above P_{C2} is very similar to that of ambient-pressure SmB_6 [Fig. 1(c)]. It is hence natural to ask whether this high-pressure gapped state is topologically nontrivial. To know the answer, we applied a magnetic field of 7 T on the sample at given pressures and find an enhancement of its resistance in the whole temperature range for the pressures ranging from 16.3 to 23.9 GPa [Figs. 3(b)–3(d)]. The similar positive magnetoresistance behaviors have been found in the TKI SmB_6 under the magnetic field below ~4.5 T, which is taken as a signature of the surface state protected by a time-reversal symmetry [21].

Another striking feature of SmB_6 is its mixed-valence state. For the valence state of YbB_6, we note that previous ARPES measurements and x-ray photoelectron experiments at ambient pressure have established that the divalent Yb component is dominant in the bulk YbB_6 [44]. To know the pressure-dependent valence state of Yb ions and especially clarify whether the high-pressure gapped phase is in a mixed-valence state, we performed high-pressure x-ray absorption measurements at beamline 14W1 at Shanghai Synchrotron Radiation Facilities. Representative L_{III}-edge XAS of YbB_6 collected at different pressures are presented in Fig. 4(a). In the pressure range investigated, the Yb^{2+} peak is clearly seen at 8939.8

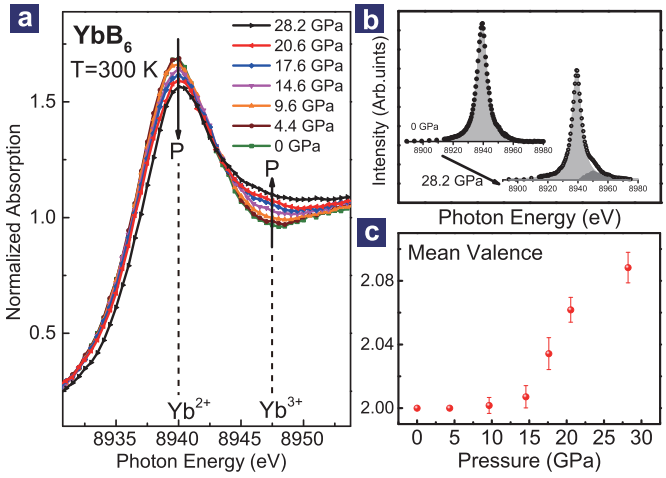

FIG. 4. (Color online) (a) XAS of Yb through the L_{III}-edge at different pressures. The dashed vertical lines indicate characteristic energy positions of the L_{III}-edge peak for Yb^{2+} and Yb^{3+}, respectively. (b) XAS of Yb measured at ambient pressure and 28.2 GPa after the background deduction. The light gray area and dark gray area represent the Yb^{2+} component and Yb^{3+} component, respectively. (c) Pressure dependence of the mean valence determined from XAS data.

eV, but no visible Yb^{3+} peak is observed at higher energies. Instead, a dip is found at 8946.3 eV where the Yb^{3+} peak usually appears. Significantly, we find that the intensity of the Yb^{2+} peak decreases upon increasing pressure, whereas the dip is gradually filled up. A careful analysis on the extended x-ray absorption spectra for the sample indicates that the pressure-induced reduction of the dip should be attributed to the growth of the Yb^{3+} component (Fig. S3 of the Supplemental Material). As shown in Fig. 4(b), the absorption spectra collected at ambient pressure and 28.2 GPa clearly demonstrate how the pressure-induced enhancement of the Yb^{3+} spectral weight compensates the observed ambient-pressure dip. Taking the mean valence of Yb at ambient pressure as $v = 2$, the pressure dependence of v [Fig. 4(c)] can be deduced from the relative intensities of the Yb^{2+} and Yb^{3+} components. We find that v remains nearly unchanged below 10 GPa, whereas it increases remarkably at pressures greater than 15 GPa where YbB_6 enters the high-pressure gapped state. These results reveal the sensitive nature of the bulk valence in YbB_6 for which Sidorov *et al.* [43] hypothesized the possible mixed-valence state at high pressure with the recommendation of L_{III}-edge XAS measurements—now performed here 24 yr later. Our high-pressure x-ray absorption measurements confirmed the bulk divalency in YbB_6 at (or near) ambient pressure and significantly discovered the onset of mixed valency at high pressure.

The achieved results, including pressure-induced gap closing and reopening, resistance plateau, positive magnetoresistance effect, and the mixed-valence state, inspire us to propose that this high-pressure gapped state in YbB_6 may be topologically nontrivial. Therefore, we denote the pressure-induced gapped state as a TNT-HP phase in the phase diagram [Fig. 3(a)]. The theoretical studies of Ref. [40] on the electronic structure of pressurized YbB_6 propose that the pressurized YbB_6 above 15 GPa may be a partially gapped semimetal. This interesting high-pressure gapped phase with topologically nontrivial features deserves further investigation.

In conclusion, we find two pressure-induced quantum phase transitions in YbB_6 from the ambient-pressure *p-d* gapped semiconducting state to the intermediate semimetallic state and then from the semimetallic state to a possible topologically nontrivial gapped state through *in situ* high-pressure transport and synchrotron x-ray diffraction measurements. Our results demonstrate that the pressure-induced semimetallic state is a pathway connecting the ambient-pressure semiconducting state and the high-pressure gapped state. Significantly, our high-pressure absorption results reveal that the mixed-valence state in pressurized YbB_6 above 15 GPa plays an important role in the development of the high-pressure gapped state.

The work in China was supported by the NSF of China (Grants No. 91321207, No. 11427805, No. 11404384, No. 11174339, and No. U1532267) and the Strategic Priority Research Program (B) of the Chinese Academy of Sciences (Grants No. XDB07020300 and No. XDB07020200). The works in the United States were supported by DARPA under Agreements No. FA8650-13-1-7374 and No. FAPESP 2013/2018-0.

[1] Liang Fu, C. L. Kane, and E. J. Mele, Phys. Rev. Lett. **98**, 106803 (2007).
[2] J. E. Moore and L. Balents, Phys. Rev. B **75**, 121306(R) (2007).
[3] X.-L. Qi, T. L. Hughes, and S.-C. Zhang, Phys. Rev. B **78**, 195424 (2008).
[4] M. Z. Hasan and C. L. Kane, Rev. Mod. Phys. **82**, 3045 (2010).
[5] X. L. Qi and S. C. Zhang, Rev. Mod. Phys. **83**, 1057 (2011).
[6] M. Konig, S. Wiedmann, C. Brune, A. Roth, H. Buhmann, L. W. Molenkamp, X. L. Qi, and S. C. Zhang, Science **318**, 766 (2007).
[7] Y. L. Chen, J. G. Analytis, J. H. Chu, Z. K. Liu, S. K. Mo, X. L. Qi, H. J. Zhang, D. H. Lu, X. Dai, Z. Fang, S. C. Zhang, I. R. Fisher, Z. Hussain, and Z. X. Shen, Science **325**, 178 (2009).
[8] H. J. Zhang, C. X. Liu, X. L. Qi, X. Dai, Z. Fang, and S. C. Zhang, Nat. Phys. **5**, 438 (2009).
[9] D.-X. Qu, Y. S. Hor, J. Xiong, R. J. Cava, and N. P. Ong, Science **329**, 821 (2010).
[10] J. S. Zhang, C. Z. Chang, P. Z. Tang, Z. C. Zhang, X. Feng, K. Li, L. L. Wang, X. Chen, C. X. Liu, W. H. Duan, K. He, Q. K. Xue, X. C. Ma, and Y. Y. Wang, Science **339**, 1582 (2013).
[11] F. Lu, J. Z. Zhao, H. Weng, Z. Fang, and X. Dai, Phys. Rev. Lett. **110**, 096401 (2013).
[12] M. Neupane, N. Alidoust, S. Y. Xu, T. Kondo, Y. Ishida, D. J. Kim, C. Liu, I. Belopolski, Y. J. Jo, T. R. Chang, H. T. Jeng, T. Durakiewicz, L. Balicas, H. Lin, A. Bansil, S. Shin, Z. Fisk, and M. Z. Hasan, Nat. Commun. **4**, 7 (2013).
[13] C.-H. Min, P. Lutz, S. Fiedler, B. Y. Kang, B. K. Cho, H. D. Kim, H. Bentmann, and F. Reinert, Phys. Rev. Lett. **112**, 226402 (2014).
[14] W. A. Phelan, S. M. Koohpayeh, P. Cottingham, J. W. Freeland, J. C. Leiner, C. L. Broholm, and T. M. McQueen, Phys. Rev. X **4**, 031012 (2014).
[15] H. M. Weng, J. Z. Zhao, Z. J. Wang, Z. Fang, and X. Dai, Phys. Rev. Lett. **112**, 016403 (2014).
[16] M. Xia, J. Jiang, Z. R. Ye, Y. H. Wang, Y. Zhang, S. D. Chen, X. H. Niu, D. F. Xu, F. Chen, X. H. Chen, B. P. Xie, T. Zhang, and D. L. Feng, Sci. Rep. **4**, 5999 (2014).
[17] N. Xu, P. K. Biswas, J. H. Dil, R. S. Dhaka, G. Landolt, S. Muff, C. E. Matt, X. Shi, N. C. Plumb, M. Radović, E. Pomjakushina, K. Conder, A. Amato, S. V. Borisenko, R. Yu, H. M. Weng, Z. Fang, X. Dai, J. Mesot, H. Ding, and M. Shi, Nat. Commun. **5**, 4566 (2014).
[18] C. Varma, Rev. Mod. Phys. **48**, 219 (1976).
[19] X. Y. Feng, J. Dai, C. H. Chung, and Q. Si, Phys. Rev. Lett. **111**, 016402 (2013).
[20] G. Li, Z. Xiang, F. Yu, T. Asaba, B. Lawson, P. Cai, C. Tinsman, A. Berkley, S. Wolgast, Y. S. Eo, D.-J. Kim, C. Kurdak, J. W. Allen, K. Sun, X. H. Chen, Y. Y. Wang, Z. Fisk, and L. Li, Science **346**, 1208 (2014).
[21] D. J. Kim, J. Xia, and Z. Fisk, Nat. Mater. **13**, 466 (2014).
[22] M. Dzero, K. Sun, V. Galitski, and P. Coleman, Phys. Rev. Lett. **104**, 106408 (2010).

[23] J. Jiang, S. Li, T. Zhang, Z. Sun, F. Chen, Z. R. Ye, M. Xu, Q. Q. Ge, S. Y. Tan, X. H. Niu, M. Xia, B. P. Xie, Y. F. Li, X. H. Chen, H. H. Wen, and D. L. Feng, Nat. Commun. **4**, 3010 (2013).

[24] S. Wolgast, Ç. Kurdak, K. Sun, J. W. Allen, D.-J. Kim, and Z. Fisk, Phys. Rev. B **88**, 180405 (2013).

[25] S. Rößler, T.-H. Jang, D.-J. Kim, L. H. Tjeng, Z. Fisk, F. Steglich, and S. Wirth, Proc. Natl. Acad. Sci. **111**, 4798 (2014).

[26] D. J. Kim, S. Thomas, T. Grant, J. Botimer, Z. Fisk, and J. Xia, Sci. Rep. **3**, 3150 (2013).

[27] J. Yong, Y. Jiang, D. Usanmaz, S. Curtarolo, X. Zhang, L. Li, X. Pan, J. Shin, I. Takeuchi, and R. L. Greene, Appl. Phys. Lett. **105**, 222403 (2014).

[28] Z. Yue, X. Wang, D. Wang, J. Wang, D. Culcer, and S. Dou, J. Phys. Soc. Jpn. **84**, 044717 (2015).

[29] F. Chen, C. Shang, Z. Jin, D. Zhao, Y. P. Wu, Z. J. Xiang, Z. C. Xia, A. F. Wang, X. G. Luo, T. Wu, and X. H. Chen, Phys. Rev. B **91**, 205133 (2015).

[30] Y. Luo, H. Chen, J. Dai, Z.-a. Xu, and J. D. Thompson, Phys. Rev. B **91**, 075130 (2015).

[31] N. Wakeham, Y. Q. Wang, Z. Fisk, F. Ronning, and J. D. Thompson, Phys. Rev. B **91**, 085107 (2015).

[32] N. Xu, C. E. Matt, E. Pomjakushina, X. Shi, R. S. Dhaka, N. C. Plumb, M. Radović, P. K. Biswas, D. Evtushinsky, V. Zabolotnyy, J. H. Dil, K. Conder, J. Mesot, H. Ding, and M. Shi, Phys. Rev. B **90**, 085148 (2014).

[33] W. T. Fuhrman, J. Leiner, P. Nikolić, G. E. Granroth, M. B. Stone, M. D. Lumsden, L. DeBeer-Schmitt, P. A. Alekseev, J.-M. Mignot, S. M. Koohpayeh, P. Cottingham, W. A. Phelan, L. Schoop, T. M. McQueen, and C. Broholm, Phys. Rev. Lett. **114**, 036401 (2015).

[34] W. Ruan, C. Ye, M. Guo, F. Chen, X. Chen, G.-M. Zhang, and Y. Wang, Phys. Rev. Lett. **112**, 136401 (2014).

[35] P. Syers, D. Kim, M. S. Fuhrer, and J. Paglione, Phys. Rev. Lett. **114**, 096601 (2015).

[36] B. S. Tan, Y.-T. Hsu, B. Zeng, M. C. Hatnean, N. Harrison, Z. Zhu, M. Hartstein, M. Kiourlappou, A. Srivastava, M. D. Johannes, T. P. Murphy, J.-H. Park, L. Balicas, G. G. Lonzarich, G. Balakrishnan, and S. E. Sebastian, Science **349**, 287 (2015).

[37] N. Xu, C. E. Matt, E. Pomjakushina, J. H. Dil, G. Landolt, J.-Z. Ma, X. Shi, R. S. Dhaka, N. C. Plumb, M. Radovic, V. N. Strocov, T. K. Kim, M. Hoesch, K. Conder, J. Mesot, H. Ding, and M. Shi, arXiv:1405.0165.

[38] M. Neupane, S.-Y. Xu, N. Alidoust, G. Bian, D. J. Kim, C. Liu, I. Belopolski, T. R. Chang, H. T. Jeng, T. Durakiewicz, H. Lin, A. Bansil, Z. Fisk, and M. Z. Hasan, Phys. Rev. Lett. **114**, 016403 (2015).

[39] E. Frantzeskakis, N. de Jong, J. X. Zhang, X. Zhang, Z. Li, C. L. Liang, Y. Wang, A. Varykhalov, Y. K. Huang, and M. S. Golden, Phys. Rev. B **90**, 235116 (2014).

[40] C.-J. Kang, J. D. Denlinger, J. W. Allen, C.-H. Min, F. Reinert, B. Y. Kang, B. K. Cho, J.-S. Kang, J. H. Shim, and B. I. Min, arXiv:1508.07212.

[41] H. K. Mao, J. Xu, and P. M. Bell, J. Geophys. Res.: Solid Earth **91**, 4673 (1986).

[42] See Supplemental Material at http://link.aps.org/supplemental/10.1103/PhysRevB.92.241118 for sample measurements.

[43] V. A. Sidorov, N. N. Stepanov, O. B. Tsiok, L. G. Khvostantsev, I. A. Smirnov, M. M. Korsukova, and A. Tybulewicz, Sov. Phys.-Solid State **33**, 720 (1991).

[44] T. Nanba, M. Tomikawa, Y. Mori, N. Shino, S. Imada, S. Suga, S. Kimura, and S. Kunii, Physica B **186**, 557 (1993).